Structural Basis for the Regulation of Protein Kinase A by Activation Loop Phosphorylation*

Jon M. Steichen[‡], Michael Kuchinskas[‡1], Malik M. Keshwani[§¶], Jie Yang[‡], Joseph A. Adams[§], and Susan S. Taylor[‡§¶2]
From the [‡]Departments of Chemistry and Biochemistry and [§]Pharmacology, and the [¶]Howard Hughes Medical Institute, University of California at San Diego, La Jolla, California 92093

Background: Activation loop phosphorylation is a conserved mechanism for regulating protein kinases.
Results: The unphosphorylated C-subunit structure of protein kinase A shows decoupling of the two lobes of the enzyme.
Conclusion: Phosphorylation orients the small and large lobes of the kinase for catalysis.
Significance: PKA in its unphosphorylated state shows a great deal of structural disorganization, and this is difficult to predict in advance.

The catalytic subunit of cAMP-dependent protein kinase (PKA) is a member of the AGC group of protein kinases. Whereas PKA has served as a structural model for the protein kinase superfamily, all previous structures of the catalytic subunit contain a phosphorylated activation loop. To understand the structural effects of activation loop phosphorylation at Thr-197 we used a PKA mutant that does not autophosphorylate at Thr-197. The enzyme crystallized in the apo-state, and the structure was solved to 3.0 Å. The N-lobe is rotated by 18° relative to the wild-type apoenzyme, which illustrates that the enzyme likely exists in a wide range of conformations in solution due to the uncoupling of the N- and C-lobes. Several regions of the protein including the activation loop are disordered in the structure, and there are alternate main chain conformations for the magnesium positioning loop and catalytic loop causing a complete loss of hydrogen bonding between these two active site structural elements. These alterations are reflected in a 20-fold decrease in the apparent phosphoryl transfer rate as measured by pre-steady-state kinetic methods.

The catalytic subunit of the cAMP-dependent protein kinase is a member of the AGC group of protein kinases. It is one of the simplest protein kinases because it contains a kinase domain with only short N- and C-terminal extensions. Additionally, it can be expressed efficiently in bacteria (1). This has made it an ideal structural and biochemical model for the protein kinase

family. One of the most common mechanisms for protein kinase regulation is the phosphorylation of a conserved residue within the activation loop of the kinase. This is generally true in the RD class of protein kinases, which includes most protein kinases. In the RD kinases the RD arginine from the catalytic loop interacts directly with the phosphate in the activation loop (2). The phosphate on the activation loop makes hydrogen bonding interactions to residues from both lobes of the enzyme which stabilizes the enzyme in an active conformation. In PKA these residues are Lys-189 and Thr-195 from the activation segment, Arg-165 from the catalytic loop, and His-87 from the C-helix (Fig. 1).

At the N terminus of the activation loop there is a conserved DFG motif, also called the magnesium positioning loop because the aspartate coordinates magnesium at the active site. This region has been found to be a common regulatory motif in protein kinases. The DFG phenylalanine packs into a hydrophobic pocket between one residue from the N-lobe and one residue from the C-lobe, thus creating a hydrophobic regulatory (R)-spine[3] (3). This packing interaction is referred to as the "DFG-in" conformation. In many kinases, inactivation occurs when this phenylalanine moves out of the hydrophobic pocket, disrupting the orientation of the DFG aspartate and in some cases sterically blocking the ATP binding site (4, 5). These are referred to as "DFG-out" conformations. Due to its proximity to the activation loop phosphorylation site, the DFG phenylalanine is the key regulatory element of the hydrophobic R-spine that bridges the N- and C-lobes of the kinase. In PKA the R-spine consists of two residues from the N-lobe (Leu-95 and Leu-106) and two residues from the C-lobe (Tyr-164 and Phe-185). All active protein kinases have the DFG-in conformation; however, inactivation does not require the DFG-out conformation. In some kinases the spine is broken in other ways such as by rotation of the C-helix (6, 7). In other kinases inactivation occurs without disruption of the spine (8). In addition to the R-spine there is a catalytic (C)-spine. The C-spine is a noncontiguous hydrophobic ensemble that also traverses both lobes of the enzyme and is completed by the adenine ring of ATP (9).

[3] The abbreviations used are: R-spine, regulatory spine; C-spine, catalytic spine; PDB, Protein Data Bank.
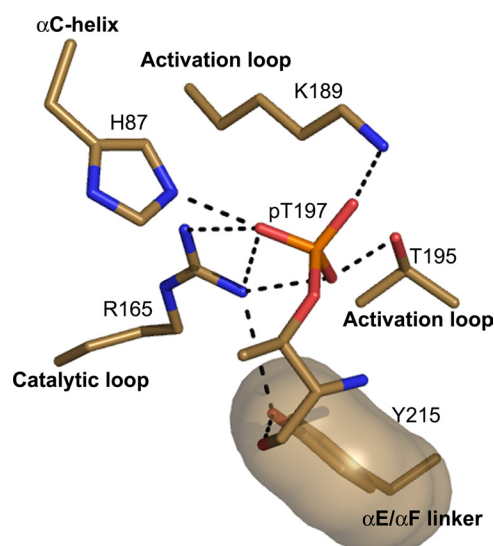
FIGURE 1. **Activation loop phosphorylation site ties together numerous regions of the protein through a hydrogen bonding network which includes the activation loop, the catalytic loop, and the αE/αF linker from the C-lobe, and the αC-helix from the N-lobe.**

Numerous protein kinases have been crystallized in the unphosphorylated state. In general, they show a high degree of diversity compared with the enzymes in their phosphorylated state. This may in part be due to the variety of ligands that have been co-crystallized with the kinase domains. The presence of a ligand in the active site may align the N- and C-lobes as well as stabilize the active site. Akt2 is the only AGC kinase that has been crystallized in the unphosphorylated, apo conformation (10). It showed a disordered C-helix, and the DFG Phe-294 occupied the ATP binding site in the DFG-out conformation. Other AGC kinases such as PDK1, co-crystallized with ATP, show only subtle structural changes even though the kinase is catalytically inactive without activation loop phosphorylation (8). This indicates that there may be dynamic changes associated with phosphorylation that are masked in the presence of ligand. In some of the more interesting cases the kinases have crystallized as dimers with the activation loops swapped (11–15). Many of the observed structural changes such as the DFG-in to DFG-out conformational change as well as the activation loop swapping occur in diverse kinases including both Ser/Thr and Tyr kinases. Therefore many of these changes may be dynamic and generally true for many kinases.

The C-subunit of PKA gets constitutively phosphorylated on both the activation loop as well as the turn motif in mammalian cells, and when expressed in bacteria it autophosphorylates on both of these sites (16). Several biochemical studies have been carried out on PKA to assess the effects of activation loop phosphorylation. The kinetic effects of mutating the activation loop Thr-197, studied previously by solvent viscosity techniques, showed that mutation of the activation loop Thr-197 to Ala or Asp primarily reduced the rate of phosphoryl transfer (17), and this was found to be generally true for protein kinases (18). It was recently shown that a mutation in the activation loop, R194A, blocks activation loop phosphorylation due to the disruption of the PKA substrate consensus sequence (19, 20). This mutant version of the C-subunit (C^{R194A}) can be stably

expressed in bacteria, and by co-expressing the mutant with PDK1 to obtain activation loop phosphorylation it was determined that the R194A mutation had little effect on the biochemical properties of the enzyme. Therefore, the mutant C^{R194A} serves as a good model for studying the biochemical changes associated with activation loop phosphorylation in PKA. The steady-state kinetics of the unphosphorylated C^{R194A} mutant were measured, and it was found to have an increased K_m for both ATP as well as kemptide (Leu-Arg-Arg-Ala-Ser-Leu-Gly) by $\sim$10-fold whereas the k_{cat} was not affected. In addition to a change in the kinetics of the enzyme it was shown that the enzyme C^{R194A} had decreased affinity for both the regulatory subunit of PKA as well as for the heat stable protein kinase inhibitor PKI (19, 20). The dynamic structural changes were also studied in C^{R194A} by hydrogen-deuterium exchange coupled to mass spectrometry, and the enzyme was found to be much more solvent-accessible in the unphosphorylated state, most significantly in regions around the activation loop such as the catalytic loop, the magnesium positioning loop, the $p + 1$ loop, and more distally the αH–αI loop (20). The unphosphorylated enzyme was also more thermolabile.

The C-subunit of PKA has been crystallized in many states including several ATP analog-bound states, inhibitory and regulatory subunit-bound states, as well as in its apo state. All structures to date, however, contain phosphate on the activation loop Thr-197. In this study we crystallized the apo, unphosphorylated PKA mutant C^{R194A} and solved the structure to 3.0-Å resolution. The two lobes of the enzyme were found to be uncoupled in the unphosphorylated protein compared with all previous PKA structures as measured by an 18° rotation of the N-lobe. This could be explained by the disruption of the hydrophobic spine that links the N- and C-lobes of the protein. Additionally, the hydrogen bonding network that integrates the active site was disrupted in the unphosphorylated enzyme. Finally, this alteration of the active site was correlated with a 20-fold reduction in the rate of phosphoryl transfer.

EXPERIMENTAL PROCEDURES

Purification and Crystallization—The His$_6$-tagged murine Cα-subunit of PKA containing mutation R194A (C^{R194A}) in pET15b was expressed in *E. coli* (BL21 (DE3)) (20). Cultures were grown at 37 °C to an A_{600} of $\sim$0.8 and induced with 0.5 mM isopropyl β-D-thiogalactopyranoside. The cultures were allowed to grow overnight at 16 °C before being harvested. The pellet was resuspended in lysis buffer (50 mM KH$_2$PO$_4$, 20 mM Tris-HCl, 100 mM NaCl, 5 mM β-mercaptoethanol, pH 8.0) and lysed using a microfluidizer (Microfluidics) at 18,000 p.s.i. The cells were clarified by centrifugation at 17,000 rpm at 4 °C for 50 min in a Beckman JA20 rotor, and the supernatant was incubated with ProBond Resin (Invitrogen) for 1 h at 4 °C. The resin was loaded onto a column and washed twice with the lysis buffer and twice with wash buffer (50 mM KH$_2$PO$_4$, 20 mM Tris-HCl, 100 mM or 1 M NaCl, 10 mM imidazole, and 5 mM β-mercaptoethanol, pH 7). An imidazole elution buffer using four different concentrations of imidazole (50, 100, 200, and 500 mM) in wash buffer was used to elute the His-tagged protein. Samples containing the most protein were dialyzed overnight into 20 mM KH$_2$PO$_4$, 20 mM KCl, and 2.5 mM DTT, pH

6.5, and then loaded onto a prepacked Mono S 10/10 (GE Healthcare) cation exchange column equilibrated in the same buffer. The protein was eluted with equilibration buffer containing a KCl gradient ranging from 0 to 1 M. In some cases it was necessary to run the protein over the ion exchange column a second time at pH 7.15 to obtain a high level of purity. The first major peak that eluted was concentrated to ~10–15 mg ml^{-1} and set up for crystallization at 4 °C using the hanging drop vapor diffusion method with well solution (100 mM Tris-HCl, 800 mM sodium formate, 10% PEG 1000, 10% PEG 8000, pH 8.5). The largest crystals were obtained from drops that had a protein/mother liquor ratio of 4:1 and appeared after ~2 weeks. The phosphorylation state of the activation loop was confirmed using a polyclonal Thr(P)-197 antibody that was raised in rabbits against the epitope peptide RVKGRTWpTL-CGTPEY (Invitrogen).

Data Collection and Refinement—The crystals were flash cooled in liquid nitrogen with cryoprotectant solution (mother liquor and 15% glycerol). Data were collected on the synchrotron beamline 8.2.2 of the Advanced Light Source, Lawrence Berkeley National Labs (Berkeley, CA). The data were integrated using HKL2000 (21). Molecular replacement was carried out using Phaser (22) with the apoenzyme structure of PKA as a search model (23) (PDB ID code 1J3H). The protein crystallized in the P3$_2$21 space group, and there were two molecules in the asymmetric unit. There was poor density for the small lobe in the initial model, and after extensive model building using COOT (24) it was determined that there was a large change in the relative orientation of the two lobes. After determining the correct orientation of the N- and C-lobes, 1RDQ (the highest resolution structure of PKA with Y204A mutation) (25) was used as a starting model after aligning its N- and C-lobes in the proper orientation. This model was further refined in COOT and Refmac5 using restrained refinement with TLS and setting noncrystallographic symmetry restraints (26). The TLS groups were defined as group1 (residues 14–126, 333–350) and group2 (residues 127–318). There was a clear break in the density of the activation loop between residues ~189 and 200, and it was taken to mean that the activation loop is disordered as is seen in many other kinases. However, near the interface of the two molecules in the asymmetric unit there is a stretch of weak density that could potentially belong to the activation loop of either molecule in the asymmetric unit. Attempts were made to model main chain into this density, but after further rounds of refinement the density did not improve in this region. The final model contained three water molecules modeled into this density. It is refined to an R_{work}/R_{free} of 25.2/28.6. There were no outliers in the Ramachandran plot as determined using MolProbity (27). The root mean square deviation between the two molecules in the asymmetric unit is 0.10 Å. The refinement statistics are shown in Table 1. The $F_o - F_c$ map (2.7σ) shown in Fig. 4*B* was calculated by deleting the activation loop and running 20 cycles of TLS refinement followed by 20 cycles of restrained refinement.

Rapid Quench Flow Experiments—Pre-steady-state kinetic measurements were made using a KinTek model RGF-3 quench flow apparatus following a previously published procedure (29). The apparatus consists of three syringes driven by a

TABLE 1
Data collection and refinement statistics

Crystal parameters	
PDB ID code	4DFY
Space group	P3$_2$21
Cell dimensions	
a (Å)	95.745
b (Å)	95.745
c (Å)	173.959
α (°)	90.0
β (°)	90.0
γ (°)	120.0
Data collection	
Molecules per asymmetric unit	2
Unique reflections	18,017 (1,121)
Redundancy	5.3 (4.8)
Resolution range (Å)	50–3.0 (3.11–3.00)^a
R_{sym} (%)	6.3 (33.2)
$I/\sigma I$	28.1 (2.8)
Completeness (%)	94.9 (59.5)
Refinement statistics	
R_{work}/R_{free} ^{b} (%)	25.2/28.6
Ramachandran angles^c (%)	
Favored regions	94.6
Allowed regions	100
Root mean square deviations	
Bond lengths (Å)	0.012
Bond angles (°)	1.3

^{a} Values in parentheses correspond to the highest resolution shell.
^{b} 5.1% of the data was excluded from the refinement to calculate the R_{free}.
^{c} Ramachandran plot quality as defined in MolProbity (27).

stepping motor. Typical experiments were performed by mixing equal volumes of the PKA in one reaction loop and [γ-^{32}P]ATP (5,000–15,000 cpm/pmol) and Kemptide in the second reaction loop all in the presence of 100 mM Mops, pH 7.4, 10 mM free Mg^{2+}, 5 mg/ml BSA. The reaction was quenched with 30% acetic acid in the third syringe, and the reactions were analyzed using the filter binding assay described above. Control experiments lacking PKA were run to define a background correction. The final concentrations of C-subunit, Kemptide, and ATP were 1, 500, and 500 μM, respectively.

RESULTS

Global Changes in Unphosphorylated Protein—Three regions in the protein were disordered in the structure: the N terminus (1–130), the activation loop (189–200), and the C-terminal tail (319–333). The turn motif site Ser-338 is phosphorylated and is similar to the wild-type enzyme. Using the C-lobe αE and αF helices for alignment, we compared the unphosphorylated enzyme with the wild-type apoenzyme in the open conformation (PDB ID code 1J3H). There is an additional 18° rotation of the N-lobe β-sheet relative to the C-lobe (Fig. 2, *A* and *B*). A C-lobe alignment to the wild-type enzyme in its closed conformation (PDB ID code 1ATP) shows a total 30° rotation of the β-sheet (Fig. 2*A*). Individually aligning the N- and C-lobes shows that there are only small changes in the overall structure of each lobe (Fig. 2, *A* and *C*). The Cα root mean square deviation between the N- (residues 40–120) and C-lobes (residues 127–290) is 0.456 and 0.644 Å, respectively. Thus, the N- and C-lobes rotate as two ridged bodies in the unphosphorylated enzyme. This rotation is greater than has been observed for other unphosphorylated AGC kinases; however, these protein kinases all have ligands bound to the ATP binding pocket with the exception of Akt2. When comparing the structure with other apo, unphosphorylated protein kinase
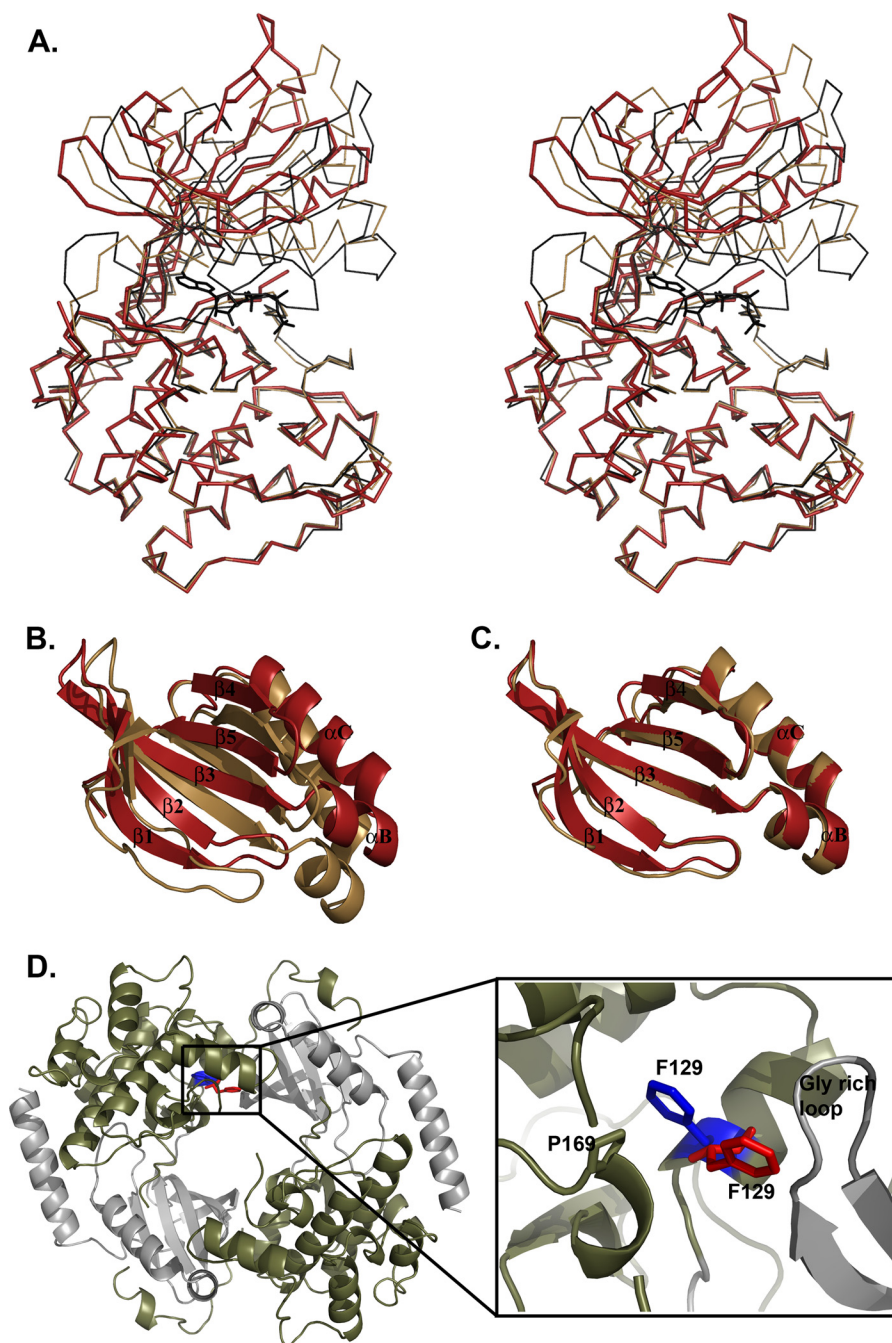
FIGURE 2. **Alignment of C^{R194A} with wild-type C-subunit.** *A*, stereo view of the apo wild-type C-subunit (1J3H; *tan*), the closed ternary complex (1ATP; *black*) with C^{R194A} (*red*) aligned along the αE and αF helices shows the similarity of the C-lobe and the rotation of the N-lobe. ATP is shown in *black*. *B*, same alignment as shown in *A* between wild-type apo and C^{R194A} but showing only the 18° rotation of the N-lobe. *C*, alignment of the β-sheet in the N-lobe between apo wild-type (*tan*) and C^{R194A} (*red*). *D*, crystal packing between the two molecules of C^{R194A} in the asymmetric unit. The C-lobe is colored *olive*, and the N-lobe is colored *gray*. The side chain of Phe-129 (shown as a *blue stick*) is rotated away from the glycine-rich loop from the other molecule of the asymmetric unit and packs against Pro-169. The position of Phe-129 in the wild-type C-subunit is shown as a *red stick*.

structures, C^{R194A} shows a domain twist similar to p38 kinase, but C^{R194A} is in a more open conformation (28).

Disruption of Hydrogen Bonding Network at Active Site—The active site of the unphosphorylated protein is dramatically different from the wild-type enzyme. Virtually every catalytic residue in the C-lobe is displaced from the wild-type active conformation (Fig. 3). Although many of these changes can be rationalized from the missing phosphate at Thr-197 and its subsequent disruption of the hydrogen bonding network that

integrates the active site, there is a crystal packing interaction that may be responsible for some of the changes. Phe-129 in the αD helix and near the hinge is rotated in the structure relative to its conformation in the wild-type protein. This is due to a packing interaction with the glycine-rich loop from the other molecule in the asymmetric unit (Fig. 2D). The new conformation of Phe-129 is packing against Pro-169 in the catalytic loop. The Cα of Pro169 has shifted ~2 Å compared with the wild-type protein. The Cα atoms in the adjacent residues Lys-168
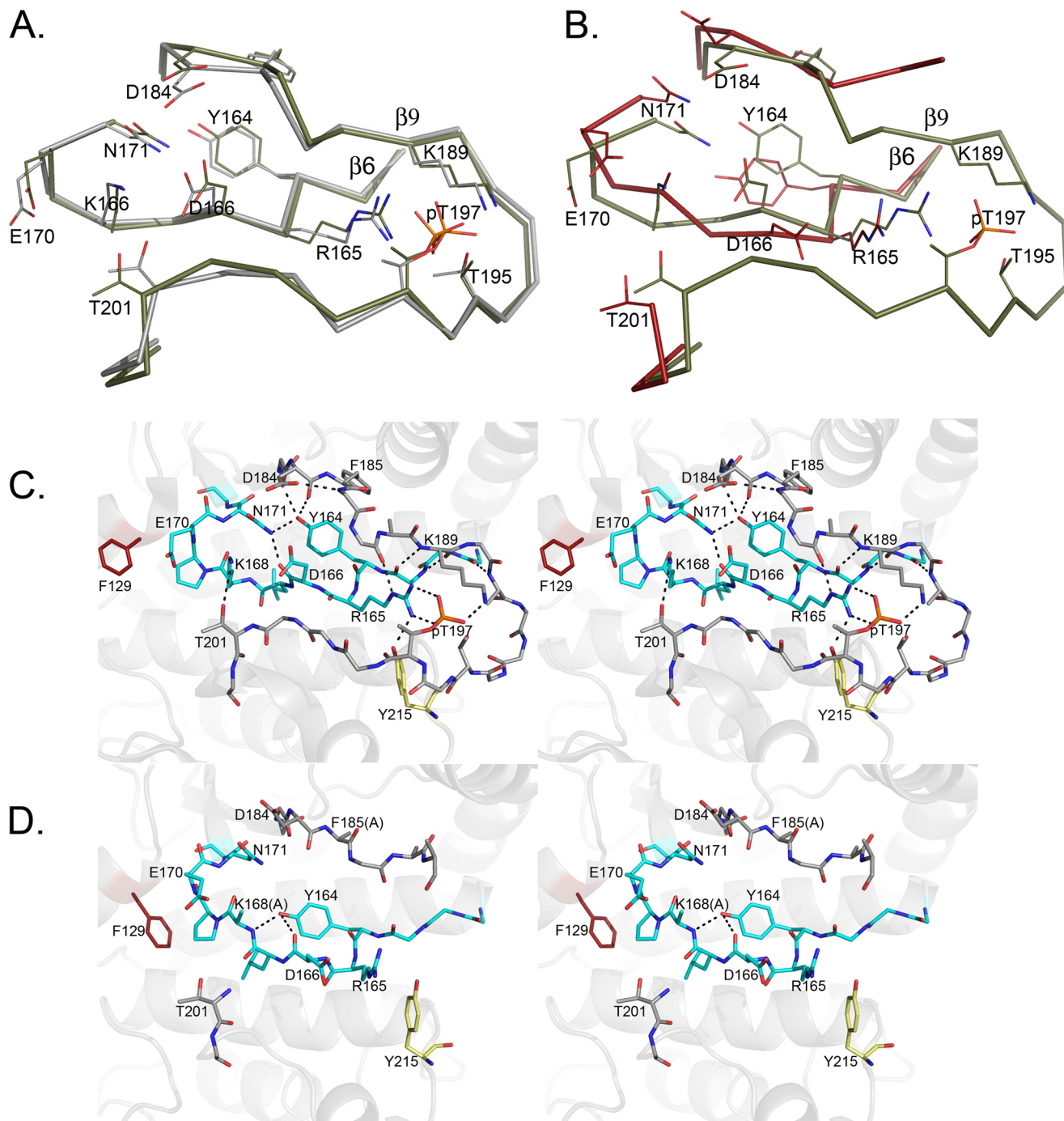
FIGURE 3. **Loss of hydrogen bonding at the active site of C^{R194A}.** *A*, alignment of wild-type apo (1J3H; *olive*) and ternary complex (1ATP; *gray*) showing that the conformation of the C-lobe portion of the active site is independent of substrate binding. *B*, alignment of the wild-type apoenzyme (*olive*) with C^{R194A} (*red*) showing the same view of the active site as in *A*. *C*, stereo view of active site of wild-type apoenzyme showing hydrogen bonds that are present in wild-type but absent in C^{R194A}. The catalytic loop is colored *teal*, and the activation loop is colored *gray*. Phe-129, which is rotated in C^{R194A} as a result of crystal packing, is shown in *red*. *D*, stereo view of the active site of C^{R194A} showing hydrogen bonds that are formed in C^{R194A} but absent in the wild-type apoenzyme. Coloring is as in *C*.

and Leu-167 are shifted ~3.5 Å and 2.3 Å, respectively (Fig. 3). Additionally it is important to note that although we are comparing the active site of the unphosphorylated enzyme with the wild-type apoenzyme in the open conformation, the conformations of the activation loop as well as the catalytic loop do not depend on substrate binding for the wild-type enzyme (Fig. 3*A*).

The activation loop is disordered from residues ~189–200 in the unphosphorylated enzyme, and the main chain starting

from the DFG-1 residue Thr-183 to Gly-186 is moved away from the catalytic loop by ~1 Å. Beyond Gly-186 the main chain makes a turn away from the catalytic loop preventing the formation of the β6:β9-sheet. Additionally, there is no electron density for most of the side chains C-terminal to the DFG Asp-184 (Fig. 4, *A* and *B*). The sum of these changes results in the loss of all hydrogen bonds bridging the activation loop to the catalytic loop (Fig. 3, *C* and *D*). The phosphate at Thr-197 can
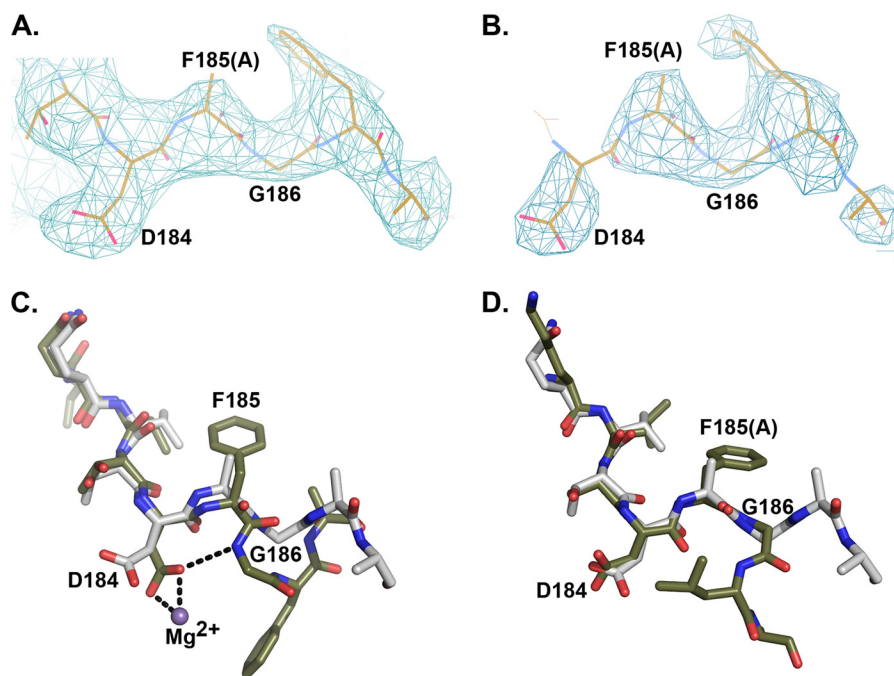
FIGURE 4. **Magnesium positioning loop shows similarity to other inactive kinases.** *A*, $2F_o - F_c$ map contoured at 1.0σ for C^{R194A} from the beginning of the activation segment to the disordered region ending at Ala-188. *B*, same view as in *A*, showing the $F_o - F_c$ map at 2.7σ after removing the activation loop from the model as described under "Experimental Procedures." *C*, same region of the activation segment as in *A* aligned with the wild-type protein (1ATP; *olive*) showing the rotation of the magnesium coordinating residue Asp-184. The magnesium ion is colored *purple*. *D*, alignment of C^{R194A} (*gray*) with the inactive form of CDK2 (1HCL; *olive*) showing a similar disruption of the hydrogen bond linking the DFG Asp-184 to the Gly-186 amide nitrogen.

make hydrogen bonds to three side chains in the open conformation and four in the closed conformation. Lys-189 belongs to β9 and forms a β-sheet with β6 directly preceding the catalytic loop. In the wild-type enzyme Lys-189 makes a hydrogen bond to the phosphate at Thr-197, and it is disordered in the unphosphorylated enzyme. Therefore this residue directly links the activation loop to the catalytic loop in the wild-type enzyme and may be responsible for the movement of the activation loop away from the catalytic loop in the unphosphorylated protein. Additionally, Arg-165 from the catalytic loop makes hydrogen-bonding interactions to the activation loop through both the phosphate at Thr-197 as well as to the main chain carbonyl oxygen of Phe-187 in the wild-type protein. In the unphosphorylated enzyme Arg-165 has moved away from the activation loop. In the wild-type enzyme, the magnesium-coordinating residue Asp-184 is held in an active conformation by making a hydrogen bond between its side chain oxygen and the main chain nitrogen of Gly-186 (Fig. 4*C*). In the unphosphorylated protein Asp-184 is turned away from Gly-186 to a catalytically incompetent conformation similar to that seen in the inactive CDK2 structure (PDB ID code 1HCL) (6) (Fig. 4*D*). The shift in the main chain at the C terminus of the catalytic loop is likely caused by the crystal-packing interaction described above where Phe-129 packs against the catalytic loop.

Hydrophobic Spine Is Broken in Unphosphorylated C-subunit—Two hydrophobic spines are a conserved feature of protein kinases in their active conformation (3). The C-spine is completed by the adenine ring of ATP whereas the regulatory R-spine is typically assembled as a consequence of phosphorylating the activation loop. The R-spine anchors the N-lobe to the C-lobe and correctly positions the catalytically important Asp-

184 of the DFG motif. In C^{R194A}, the R-spine is broken and the N-lobe is open as well as rotated substantially more than any other PKA structure (Fig. 5). The spine residue Phe-185 of the DFG motif is disordered in the structure, and Ala was modeled in its place (Fig. 4, *A* and *B*). In the wild-type structure, Phe-185 makes hydrophobic packing interactions with both Leu-95 from the N-lobe and Tyr-164 from the C-lobe. The positions of both Leu-95 and Tyr-164 are different from wild-type C. Leu-95 is in a conformation similar to wild type, but the rotation of the N-lobe has moved its position away from Phe-185 in the C-lobe. In the wild-type C-subunit the side chain of Tyr-164 in the catalytic loop is within hydrogen bonding distance to the main chain carbonyl oxygens of Asp-184 and Thr-183, and the side chain nitrogen of Asn-171. In C^{R194A} all three of these residues are out of hydrogen bonding distance, and the Tyr-164 hydroxyl group has moved by ~3 Å, losing its hydrophobic packing interaction with Phe-185 but forming new hydrogen bonds with the main chain carbonyl oxygen of Asp-166 and main chain nitrogen of Lys-168 (Fig. 3*D*). Thus, the movement of the activation loop away from the catalytic loop may have the effect of breaking the hydrophobic interaction between Tyr-164 and Phe-185, causing disorder of the side chain of Phe-185 and allowing the rotation of the N-lobe.

Rate of Phosphoryl Transfer Step in C^{R194A} Is Diminished— Because the R194A mutant altered the positions of numerous residues thought to be important for optimal catalytic function, we measured the phosphoryl transfer rate constant using rapid quench flow methods to determine whether there is a direct correlation between these disturbances and serine phosphorylation. The kinetics of the wild-type enzyme was previously shown to be biphasic (29) where the first pre-steady-state expo-
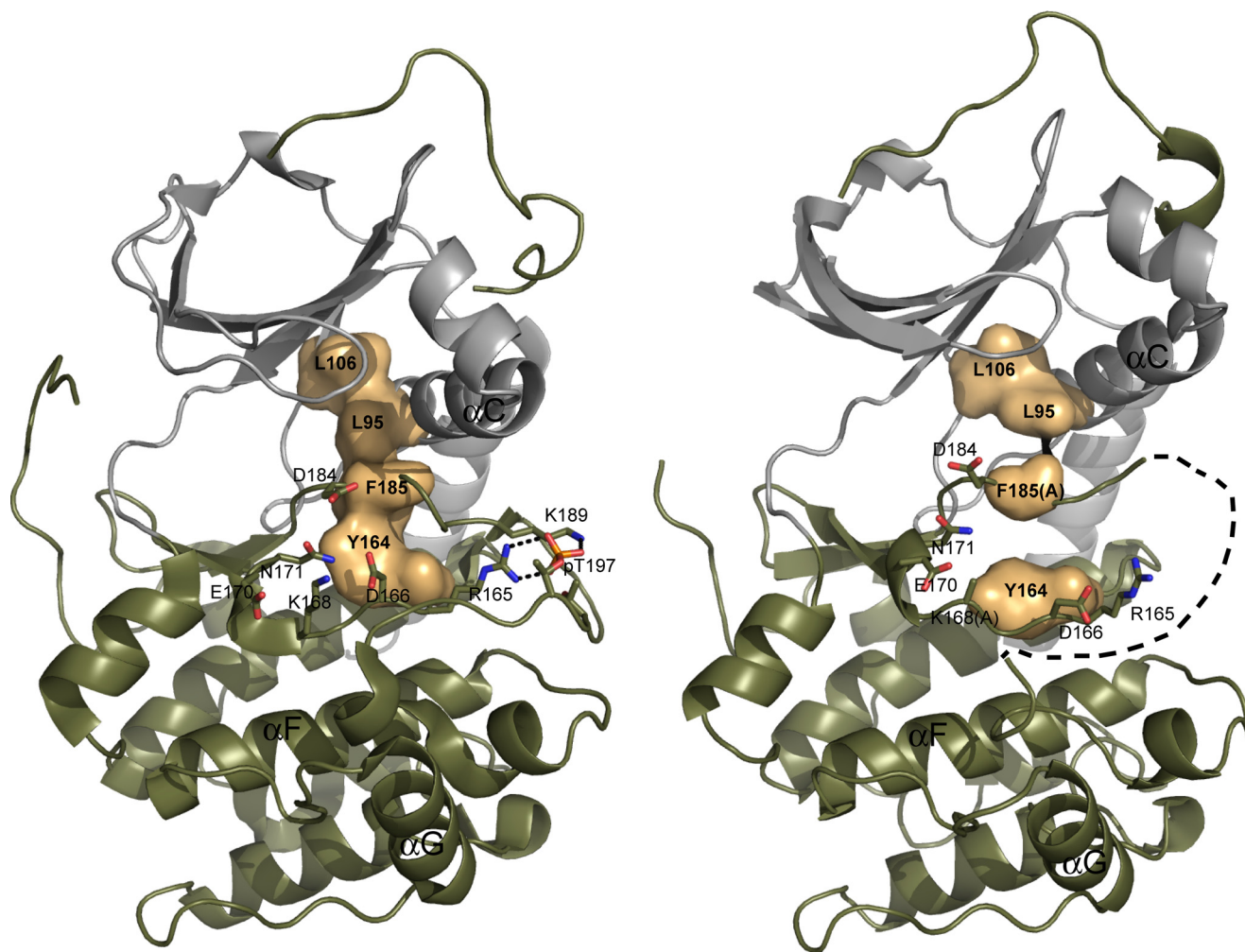
FIGURE 5. **Disruption of hydrophobic spine in C^R194A.** The hydrophobic spine is shown for the wild-type apoenzyme (1J3H; *left*), and C^R194A (*right*). The C-lobe is colored *olive*, and the N-lobe is colored *gray*. The spine is shown as a *tan* surface, and IP20 peptide is colored *teal*.

nential phase (burst) represents the rapid phosphoryl group transfer step and the second linear phase represents the rate-limiting release of ADP. We confirmed that the wild-type enzyme gave a biphasic curve with a burst rate constant of 78 s^{-1} and a linear rate constant of 13 s^{-1}. Unlike the wild-type enzyme, no exponential burst phase was observed in C^R194A, and instead it displayed a linear phase with a rate constant of 3.6 s^{-1} (Fig. 6). To ensure that the absence of burst phase is not the result of weak substrate binding, pre-steady-state kinetic experiments were repeated using higher Kemptide concentrations (2 mM) (data not shown). Under these conditions no measureable burst phase was detected, indicating that the observed changes in the kinetic profiles are likely the result of a 20-fold reduction in the phosphoryl transfer rate constant.

DISCUSSION

By crystallizing the R194A mutant of the PKA C-subunit we were able to compare the structural consequences of removing this single phosphate from the activation loop without altering the rest of the protein, including Thr-197 and the phosphorylated Ser-338. Changes were seen in the global conformation, in the hydrogen bonding network at the active site, and in the hydrophobic regulatory spine. In addition, we used a rapid

quench flow assay to define the kinetic consequences of removing the activation loop phosphate.

We previously used hydrogen-deuterium exchange to compare the dynamics of the C^R194A mutant with the wild-type C-subunit in solution (20). It was found that a peptide containing the DFG motif 182–186 exchanged ~2 amide hydrogens at a faster rate in C^R194A compared with the wild-type C-subunit, and this exchange occurred within 10 s (the first measured time point). The crystal structures show that there are two changes to the main chain amides on this peptide when comparing the wild-type and C^R194A apoenzymes. In the wild-type structure, the side chain of Asp-184 makes a hydrogen bond to the main chain amide nitrogen of Gly-186. For the amide hydrogen of Gly-186 to exchange with the solvent, the hydrogen bond must break. In the structure of C^R194A, the side chain of Asp-184 is turned away from Gly-186, and the backbone amide of Gly-186 is free to exchange with the solvent. Additionally, the amide nitrogen of Phe-186 is hydrogen bonded to the side chain of Glu-91 from the C-helix in the apo wild-type structure. Due to the rotation of the N-lobe in C^R194A this interaction is also broken. This could explain the increased rate of hydrogen exchange on this peptide in the solution study. The catalytic loop peptide (residues 163–172) was also shown to exchange at
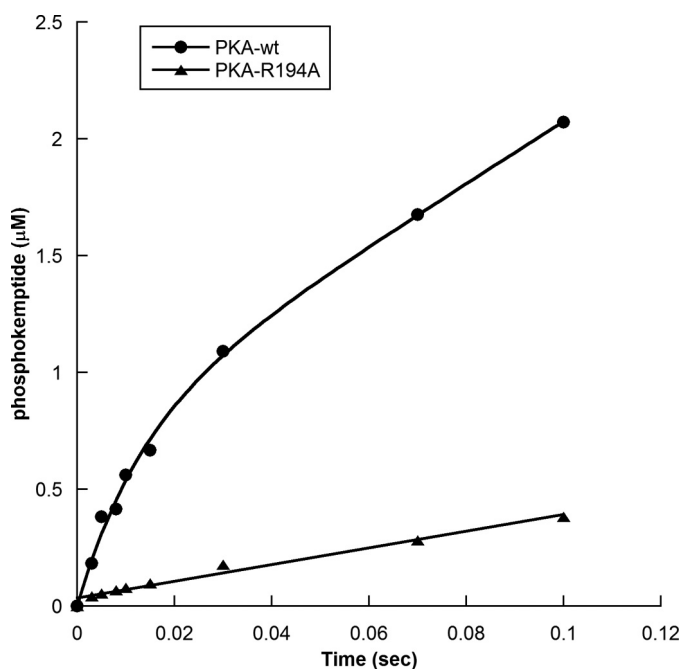
FIGURE 6. **Kinetic analysis shows a loss of pre-steady-state burst phase in the unphosphorylated C-subunit.** The first 100 ms of the phosphorylation of Kemptide by the wild-type C-subunit and C^{R194A} were measured using the rapid quench flow methods described under "Experimental Procedures."

a faster rate in the unphosphorylated enzyme. In this peptide 6–7 amide hydrogens exchanged over the course of 50 min in C^{R194A} compared with 4 amides exchanged in the wild-type protein. The resolution of the deuterium exchange study was not high enough to assign specific residues to the increased exchange rates, and furthermore, there is a crystal-packing contact in this region in the C^{R194A} structure. However, we do see a dramatic loss of hydrogen bonding between side chains of the catalytic loop and the main chain of the activation loop in the C^{R194A} structure which may explain the increased dynamics of the catalytic loop. Additionally, we showed that β6 had a faster rate of hydrogen exchange in C^{R194A} compared with the wild-type enzyme. In the wild-type C-subunit β6 and β9 form a β-sheet. Lys-189 belongs to β9, and its side chain makes a hydrogen bond with the phosphate at Thr-197. In the structure of C^{R194A} Lys-189 is disordered which explains the increased rate of hydrogen exchange in β6. Several mutants of PKA have been characterized by hydrogen-deuterium exchange and were found to be more dynamic in similar regions as the unphosphorylated enzyme. However, when these mutants were co-crystallized with MgATP and IP20 they did not show significant changes compared with the wild-type enzyme (25, 30, 31). The structure of the apo, unphosphorylated enzyme provides insight into the unstable regions of the protein that would otherwise be masked in the presence of ligand.

In the C^{R194A} structure the disassembled hydrophobic R-spine is not analogous to the DFG-out conformation in which the phenylalanine blocks the ATP binding site but is more similar to p38 kinase (PDB ID code 1WFC). In p38 kinase the rotation of the N-lobe breaks the interactions of Phe-169 with Leu-75, but its hydrophobic interaction with the C-lobe (His-148) remains intact. In PKA, Phe-185 has lost hydropho-

bic interactions from above and below, and its side chain is disordered. The main chain does not turn into the ATP binding pocket but rather moves away from the catalytic loop. This has the effect of decoupling the two lobes of the enzyme and hence a greater twist than has been observed in any previous structure of PKA. Although the ATP binding site is not sterically blocked, the N-lobe must undergo a 30° rotation to form the active or closed conformation that is characteristic of the ATP-bound ternary complex. Because C^{R194A} is not catalytically dead it must be able to rotate to the wild-type closed conformation, and therefore, multiple conformations must exist in solution. Although this structure is in good agreement with our previous solution data it represents only one conformation that could be stably incorporated into a crystal lattice.

Numerous catalytic residues are displaced in the unphosphorylated C-subunit, and this appears to correlate with a large decrease in the rate of phosphoryl transfer as measured by pre-steady-state kinetic methods. The C^{R194A} mutant shows a kinetic defect similar to the C^{T197A} mutant which has the phosphorylation site mutated to an alanine. This mutant was previously analyzed by solvent viscosity techniques (17). It showed a more severe kinetic defect compared with the R194A mutant, emphasizing the importance of the threonine hydroxyl group in stabilizing the active site, but consistent with C^{R194A} it was primarily defective in the phosphoryl transfer step. It will be interesting to see how the regulation of individual rate constants can play a role in phosphorylation within the context of macromolecular complexes where a large turnover is not required for a biological response.

The structure we present here represents a novel conformation for a kinase lacking activation loop phosphorylation. Given that protein kinases belong to one of the largest families of enzymes in the human genome it would be of great value to predict accurately the effects of activation loop dephosphorylation on individual protein kinases. PKA is closely related to other AGC kinases whose structures have been solved in their unphosphorylated states, and yet there is a great deal of dissimilarity between these structures. Perhaps in some cases the unphosphorylated conformations reflect differences in recognition requirements for the kinases that phosphorylate them. Because unphosphorylated kinases show greater structural diversity compared with the phosphorylated structures, targeting the unphosphorylated enzymes *in vivo* can be used as an alternate approach to designing selective inhibitors, and further studies are warranted.

REFERENCES

1. Herberg, F. W., Bell, S. M., and Taylor, S. S. (1993) Expression of the catalytic subunit of cAMP-dependent protein kinase in *Escherichia coli*: multiple isozymes reflect different phosphorylation states. *Protein Eng.* **6,** 771–777
2. Johnson, L. N., Noble, M. E., and Owen, D. J. (1996) Active and inactive protein kinases: structural basis for regulation. *Cell* **85,** 149–158

3. Kornev, A. P., Haste, N. M., Taylor, S. S., and Eyck, L. F. (2006) Surface comparison of active and inactive protein kinases identifies a conserved activation mechanism. *Proc. Natl. Acad. Sci. U.S.A.* **103,** 17783–17788

4. Pargellis, C., Tong, L., Churchill, L., Cirillo, P. F., Gilmore, T., Graham, A. G., Grob, P. M., Hickey, E. R., Moss, N., Pav, S., and Regan, J. (2002) Inhibition of p38 MAP kinase by utilizing a novel allosteric binding site. *Nat. Struct. Biol.* **9,** 268–272

5. Hubbard, S. R., Wei, L., Ellis, L., and Hendrickson, W. A. (1994) Crystal structure of the tyrosine kinase domain of the human insulin receptor. *Nature* **372,** 746–754

6. Schulze-Gahmen, U., De Bondt, H. L., and Kim, S. H. (1996) High-resolution crystal structures of human cyclin-dependent kinase 2 with and without ATP: bound waters and natural ligand as guides for inhibitor design. *J. Med. Chem.* **39,** 4540–4546

7. Huse, M., and Kuriyan, J. (2002) The conformational plasticity of protein kinases. *Cell* **109,** 275–282

8. Komander, D., Kular, G., Deak, M., Alessi, D. R., and van Aalten, D. M. (2005) Role of T-loop phosphorylation in PDK1 activation, stability, and substrate binding. *J. Biol. Chem.* **280,** 18797–18802

9. Kornev, A. P., and Taylor, S. S. (2010) Defining the conserved internal architecture of a protein kinase. *Biochim. Biophys. Acta* **1804,** 440–444

10. Huang, X., Begley, M., Morgenstern, K. A., Gu, Y., Rose, P., Zhao, H., and Zhu, X. (2003) Crystal structure of an inactive Akt2 kinase domain. *Structure* **11,** 21–30

11. Oliver, A. W., Paul, A., Boxall, K. J., Barrie, S. E., Aherne, G. W., Garrett, M. D., Mittnacht, S., and Pearl, L. H. (2006) Trans-activation of the DNA-damage signalling protein kinase Chk2 by T-loop exchange. *EMBO J.* **25,** 3179–3190

12. Oliver, A. W., Knapp, S., and Pearl, L. H. (2007) Activation segment exchange: a common mechanism of kinase autophosphorylation? *Trends Biochem. Sci.* **32,** 351–356

13. Lee, S. J., Cobb, M. H., and Goldsmith, E. J. (2009) Crystal structure of domain-swapped STE20 OSR1 kinase domain. *Protein Sci.* **18,** 304–313

14. Sunami, T., Byrne, N., Diehl, R. E., Funabashi, K., Hall, D. L., Ikuta, M., Patel, S. B., Shipman, J. M., Smith, R. F., Takahashi, I., Zugay-Murphy, J., Iwasawa, Y., Lumb, K. J., Munshi, S. K., and Sharma, S. (2010) Structural basis of human p70 ribosomal S6 kinase-1 regulation by activation loop phosphorylation. *J. Biol. Chem.* **285,** 4587–4594

15. Pike, A. C., Rellos, P., Niesen, F. H., Turnbull, A., Oliver, A. W., Parker, S. A., Turk, B. E., Pearl, L. H., and Knapp, S. (2008) Activation segment dimerization: a mechanism for kinase autophosphorylation of non-consensus sites. *EMBO J.* **27,** 704–714

16. Yonemoto, W., Garrod, S. M., Bell, S. M., and Taylor, S. S. (1993) Identification of phosphorylation sites in the recombinant catalytic subunit of cAMP-dependent protein kinase. *J. Biol. Chem.* **268,** 18626–18632

17. Adams, J. A., McGlone, M. L., Gibson, R., and Taylor, S. S. (1995) Phosphorylation modulates catalytic function and regulation in the cAMP-dependent protein kinase. *Biochemistry* **34,** 2447–2454

18. Adams, J. A. (2003) Activation loop phosphorylation and catalysis in protein kinases: is there functional evidence for the autoinhibitor model? *Biochemistry* **42,** 601–607

19. Moore, M. J., Kanter, J. R., Jones, K. C., and Taylor, S. S. (2002) Phosphorylation of the catalytic subunit of protein kinase A: autophosphorylation *versus* phosphorylation by phosphoinoside-dependent kinase-1. *J. Biol. Chem.* **277,** 47878–47884

20. Steichen, J. M., Iyer, G. H., Li, S., Saldanha, S. A., Deal, M. S., Woods, V. L., Jr., and Taylor, S. S. (2010) Global consequences of activation loop phosphorylation on protein kinase A. *J. Biol. Chem.* **285,** 3825–3832

21. Otwinowski, Z., and Minor, W. (1997) *Methods Enzymol.* **276,** 307–326

22. McCoy, A. J., Grosse-Kunstleve, R. W., Adams, P. D., Winn, M. D., Storoni, L. C., and Read, R. J. (2007) Phaser crystallographic software. *J. Appl. Crystallogr.* **40,** 658–674

23. Akamine, P., Madhusudan, Wu, J., Xuong, N. H., Ten Eyck, L. F., and Taylor, S. S. (2003) Dynamic features of cAMP-dependent protein kinase revealed by apoenzyme crystal structure. *J. Mol. Biol.* **327,** 159–171

24. Emsley, P., and Cowtan, K. (2004) COOT: model-building tools for molecular graphics. *Acta Crystallogr. D Biol. Crystallogr.* **60,** 2126–2132

25. Yang, J., Ten Eyck, L. F., Xuong, N. H., and Taylor, S. S. (2004) Crystal structure of a cAMP-dependent protein kinase mutant at 1.26A: new insights into the catalytic mechanism. *J. Mol. Biol.* **336,** 473–487

26. Murshudov, G. N., Vagin, A. A., and Dodson, E. J. (1997) Refinement of macromolecular structures by the maximum-likelihood method. *Acta Crystallogr. D Biol. Crystallogr.* **53,** 240–255

27. Davis, I. W., Leaver-Fay, A., Chen, V. B., Block, J. N., Kapral, G. J., Wang, X., Murray, L. W., Arendall, W. B., 3rd, Snoeyink, J., Richardson, J. S., and Richardson, D. C. (2007) MolProbity: all-atom contacts and structure validation for proteins and nucleic acids. *Nucleic Acids Res.* **35,** W375–383

28. Wilson, K. P., Fitzgibbon, M. J., Caron, P. R., Griffith, J. P., Chen, W., McCaffrey, P. G., Chambers, S. P., and Su, M. S. (1996) Crystal structure of p38 mitogen-activated protein kinase. *J. Biol. Chem.* **271,** 27696–27700

29. Grant, B. D., and Adams, J. A. (1996) Pre-steady-state kinetic analysis of cAMP-dependent protein kinase using rapid quench flow techniques. *Biochemistry* **35,** 2022–2029

30. Yang, J., Garrod, S. M., Deal, M. S., Anand, G. S., Woods, V. L., Jr., and Taylor, S. (2005) Allosteric network of cAMP-dependent protein kinase revealed by mutation of Tyr-204 in the P+1 loop. *J. Mol. Biol.* **346,** 191–201

31. Yang, J., Wu, J., Steichen, J. M., Kornev, A. P., Deal, M. S., Li, S., Sankaran, B., Woods, V. L. Jr., and Taylor, S. S. (2012) A conserved glu-arg salt bridge connects coevolved motifs that define the eukaryotic protein kinase fold. *J. Mol. Biol.* **415,** 666–679